Transmitter-RMS-Optimized Digital Pre-Emphasis for Bandwidth-limited Channels

Wing Chau Ng
Optical System Competency Centre
Huawei Technologies Co., Ltd.
Ottawa, ON K2K 3J1, Canada
wing.chau.ng@huawei.com

Qingyi Guo
Optical System Competency Centre
Huawei Technologies Co., Ltd.
Ottawa, ON K2K 3J1, Canada
qingyi.guo@huawei.com

Junho Chang
Optical System Competency Centre
Huawei Technologies Co., Ltd.
Ottawa, ON K2K 3J1, Canada
junho.chang@huawei.com

Meng Qiu, Bofang Zheng
B&P Laboratory
Huawei Technologies Co., Ltd.
Shenzhen, China
meng.qiu@huawei.com

Xuefeng Tang, Zhiping Jiang
Optical System Competency Centre
Huawei Technologies Co., Ltd.
Ottawa, ON K2K 3J1, Canada
xuefeng.Tang@huawei.com

Chuandong Li
Optical System Competency Centre
Huawei Technologies Co., Ltd.
Ottawa, ON K2K 3J1, Canada
chuandong.li@huawei.com

***Abstract*—We theoretically derive a digital pre-emphasis filter for the first time to optimize among ISI, ENoB and RMS, and experimentally show that our solution avoids RMS loss, enhancing SNR for strong pre-emphasis.**

Keywords—Digital pre-emphasis, signal processing

I. INTRODUCTION

The next-generation high-speed optical coherent transceivers suffer from transmitter (Tx) impairments such as limited bandwidth (BW), noise from RF chain, limited digital-to-analog converter (DAC) resolution and limited power to avoid saturation (or Tx nonlinearity) [1]. The electrical responses of XI, XQ, YI and YQ (called S21) should be compensated to mitigate intersymbol interference (ISI). A linear equalizer at receiver (Rx) enhances the electrical and link noise simultaneously, while digital pre-emphasis (DPE), enhancing high frequency content, increases signal's peak-to-average power ratio (PAPR) and reduces its root mean square (RMS) (or power), which eventually degrades the available signal-to-noise ratio (SNR) [1-3]. Fig. 1a shows the phenomenological interplay among ISI / post equalization enhanced noise (PEEN), RMS, and quantization [4], based on the well-known nth root method[a] [5], in which the DPE filter is in the form of $1/|C(f)|^{\beta}, 0 \le \beta \le 1$, where $C(f)$ is the Tx S21 or channel response $C(f)$, β is the "strength" of DPE. Tx's limited RMS (green) prohibits a full DPE ($\beta = 1$). For very narrow filtering, limited ENoB (blue dash-dotted), e.g. below 5 bits, further drives DPE away from the strong DPE region (which is defined as $\beta > 0.5$ here) [4].

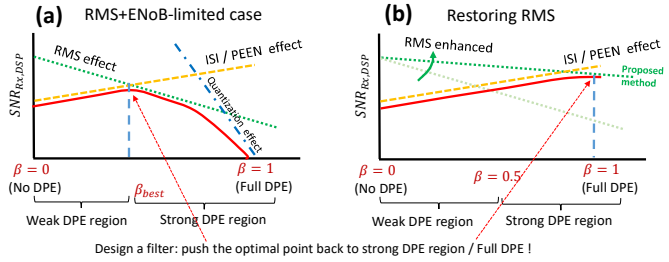

Fig. 1. Phenomenological explanation of the goal of DPE filter design. The x-axis adopts the definition of β in [5]: the nth root of the zero forcing filter[a]. β = 0 means zero DPE, β = 1 means a full DPE and partial DPE otherwise.

The state-of-the-art DPE optimization can be classified into two types. The first type considers both Tx DPE and Rx DSP to maximize signal-to-noise ratio (SNR) or minimize the error or noise of Rx-DSP, corresponding to location B in Fig. 2, subject to certain constraints. Examples include Rx-zero-forcing (ZF) [5, 6], and Rx-minimum mean square error (MMSE) [7]. Given a Tx S21 or channel response $C(f)$ and a Rx-ZF filter, refs. [5] and [6] separately claim that the optimal DPE filter shape should be $1/|C(f)|^{2/3}$, and $1/|C(f)|^{1/2}$, respectively, based on "filter-sum constraint" and "filter energy constraint" (or RMS constraint), separately supported by their simulation and experimental results. Several experimental works [4, 7], however, contradict their findings, and an empirical scan in β is required since RMS loss and quantization effect contribute to SNR degradation [4].

The second type of DPE optimization considers only Tx DPE, in an attempt to maximize the SNR before Rx DSP [8], corresponding to location A in Fig. 2. This could be justified by the "data processing inequality" in information theory that Rx DSP does not further increase the information content. Ref. [8] employed a Tx-MMSE approach without constraints, which only minimizes ISI and quantization noise. The solution converges to a ZF filter for negligible quantization, which is impossible since ZF, leading to high PAPR, requires large RMS reduction to avoid driver nonlinearity, in practice.

In view of driver nonlinearity, the Tx RMS (or power) constraint is indispensable. Limiting RMS also confines PAPR at the same time [7, 8]. Moreover, signal power constraint is conventionally applied to derive the theoretical channel capacity. A recently proposed cutoff method [4] even shows that by avoiding high-frequency components, the pre-emphasized signal's RMS can be restored to avoid SNR degradation, achieving strong pre-emphasis. Is there any mathematical interpretation or insight to shape the high-frequency content of the pre-emphasized signal?

The goal of this work is to design a DPE filter with a more self-contained interpretation based on the interplay between ISI, RMS and ENoB [4], in order to push back the optimal point to the strong DPE region, shown in Fig. 1b, such that ISI is minimized before Rx DSP, and Rx noise enhancement can thus be minimized; the channel capacity before Rx DSP is also thereby maximized by restoring in-band signal power. This work starts from the second type of DPE (maximizing SNR before Rx DSP, location A in Fig. 2) and, for the first time, analytically optimizes[b] DPE by adding a RMS constraint[c], or "filter power constraint", as indicated in green dashed lines in Fig. 1b, such that signal's RMS can be restored to approach a full DPE (β = 1) .While other works [1-5] only consider DPE within $\pm B/2$, here the proposed DPE filter is applied over the entire signal bandwidth $\pm(1+\alpha)B/2$, where α is the raised cosine (RC) roll off factor, and B is the symbol rate.

[a] There is no mathematical explanation for the nth root approach [5, 6]; it was conventionally employed to illustrate the "degree of DPE" or the "strength" of DPE.
[b] Based on the method of Lagrange multipliers.
[c] Filter energy constraint, power constraint and RMS constraint are interchangeable in this work.

The organization of this work is as follows: Section II.A provides the definitions of the model under consideration. Section II.B and II.C review the constraint-optimized Rx-ZF [5,6] and Tx-MMSE (without constraint) [8] to provide readers with sufficient background. Section II.D illustrates our proposed method. Experimental results are reported in Section III. Section IV concludes this work.

II. Defintions and Constraint Optimization Theory

A. Channel Model

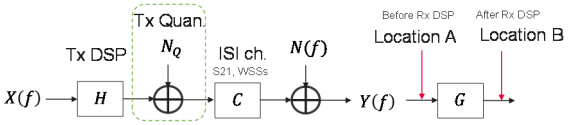

Fig. 2. Channel model. H: Tx DPE filter, C: physical ISI channel, G: Rx-DSP filter.

The time-domain channel (denoted by lowercase letters), before Rx DSP, is defined as

$$y = c * h * x + c * n_q + n, \tag{1}$$

where x is the channel input (QAM signals), h is the DPE filter, n is the overall additive colored noise, n_q is the quantization noise, c is the channel impulse response, which include all Tx, optical and Rx responses. y is the channel output before the Rx DSP. Signal, quantization noise, and channel additive noise are assumed statistically independent, i.e., $x \perp n_q \perp n$. The sign, $*$, denotes the convolution in time. The channel in frequency domain (denoted by uppercase letters) is

$$Y(f) = C(f)H(f)X(f) + C(f)N_Q + N(f). \tag{2}$$

Here white quantization noise is assumed, whose PSD is flat, i.e., $S_Q = \sigma_q^2/BW$, where BW is the DSP bandwidth, and σ_q^2 is the quantization noise variance. The distribution is assumed uniform, such that $\sigma_q^2 = \Delta_q^2/12$, where $\Delta_q = \frac{(h*x)_{max}}{2^{n_b}-1}$. A narrower filtering, C,causes a larger peak value of pre-emphasized signal, $(h*x)_{max}$, and thus higher S_Q. The assumption from [8] is adopted in this work: the peak value is proportional to the signal power, i.e., $[(h*x)_{max}]^2 = k\sigma_{h*x}^2 = k\int|H|^2 S_X(f')df'$, where k is a variable depending on the maximum PAPR. Thus, the flat PSD of the quantization noise becomes $S_Q = \frac{k\sigma_{h*x}^2}{12(2^{n_b}-1)^2 BW} = \frac{k\int|H|^2 S_X(f')df'}{12(2^{n_b}-1)^2 BW}$ and the variance of $c * n_q$ is $S_Q \int|C|^2 df$.

B. Tx-DPE with Rx-ZF

The first type of DPE optimization requires both Tx DPE and Rx DSP to maximize the SNR at location B in Fig. 2. For negligible quantization effect, ref. [5] optimizes DPE based on ZF at Rx, i.e., $G = 1/HC$, using Cauchy-Schwarz Inequality. In fact, one could revisit the optimization using "constant power/RMS constraint", $\int|H|^2\, df \le p_e$. The filter energy, p_e, is not necessarily unity, but depends on the actual Tx power without causing driver's saturation. The objective function of Rx-ZF under RMS constraint becomes

$$J_{ZF,RMS} = \int \left|\frac{1}{HC}\right|^2 S_N(f)df + \lambda[\int|H|^2\, df - p_e], \tag{3}$$

where the first term is the PEEN caused by G, while the second term is the RMS constraint. Minimizing $J_{ZF,RMS}$ results in H in the form of $1/|C(f)|^{\frac{1}{2}}$. Instead, refs. [4, 6-7] employ the form $1/|C(f)|^{\beta}$ (called the nth root method here) because a scan in β shows that 0.5 is not optimal. Namely, finite ENoB makes β smaller, while DPE bandwidth (i.e., avoiding high-frequency enhancement) makes β larger [4] thanks to RMS restoration, shown as green in Fig. 1b.

C. Tx MMSE-DPE under finite ENoB

The second type of DPE optimization requires only Tx DPE filter design to maximize the SNR at location A in Fig. 2. Intuitively, Rx DSP could enhance noise tremendously in the weak DPE region ($\beta < 0.5$) since the residual ISI is substantial. Strong DPE is thus always preferred, and revives our interest to mitigate as much as channel ISI before the Rx DSP. From the perspective of information theory, data processing inequality tells us that information content after Rx DSP can never exceed that before Rx DSP. Here, ref. [8] will be revisited to provide a sufficient background for the next section. Now, let us define error, $e = y - x$, at location A in Fig. 2. The MSE is

$$\sigma_e^2 = \int|HC-1|^2 S_X(f)\, df + \frac{k\int|H|^2 S_X(f')df'}{12(2^{n_b}-1)^2 BW}\int|C|^2 df + \int S_N(f)df, \tag{4}$$

where the first term on RHS is the residual ISI (but not called PEEN since Rx-DSP is not involved), the second is the quantization noise after the channel, and the last is the channel noise. Ref. [8] suggests that the integral over f in the second term is a constant, i.e., $p_c = \int|C|^2 df$. An optimal H can be obtained by minimizing the MSE, i.e, $\partial\sigma_e^2/\partial H = 0$, and

$$\frac{\partial}{\partial H}|HC-1|^2 S_X + \lambda_1 p_c \frac{\partial}{\partial H}|H|^2 = 0, \ \forall f, \tag{5}$$

where $\lambda_1 = \frac{k\, S_X}{12(2^{n_b}-1)^2 BW}$. The last term of σ_e^2 in (4) thus disappears, since DPE optimization without Rx-DSP does not require channel noise statistics. Thus, the optimal H becomes

$$H_{\sigma_e^2}(f) = \frac{C^*(f)S_X(f)}{|C(f)|^2 S_X(f)+\lambda_1 p_c}. \tag{6}$$

The above, however, may not be self-contained: First, eqn. (6) converges to ZF for high ENoB ($\lambda_1 = 0$) [8], which is impractical since ZF causes substantial RMS reduction to avoid driver nonlinearity as previously discussed [4]. A power constraint is therefore required. Second, the above derivation may not be mathematically sound because the quantization noise is also filtered by $C(f)$. The second term of σ_e^2 in (4) consists of two distinct integrals respectively over f and f', while the above optimization assumes constant $\int|C|^2 df$ [8]. Strictly speaking, eq. (5) should be written as,

$$\frac{\partial}{\partial H}|HC-1|^2 S_X + \frac{\partial}{\partial H}\lambda_1 \int|H|^2 df'\,|C|^2 = 0, \ \forall f, \tag{7}$$

in which H may not have a closed form.

D. Tx MMSE-DPE under finite ENoB and RMS control

In this section, we highlight our difference compared to the Tx-MMSE DPE that includes only finite ENoB [8]: for negligible quantization noise, ref. [8] does not apply any constraints, and the optimal filter in (6) becomes a ZF filter as a result, causing driver nonlinearity. RMS control has not been

explored for Tx-MMSE DPE given a limited electrical power to guarantee driver's linear operation. The contribution of this work is to design a DPE filter based on our ISI, RMS and ENoB shown in Fig. 1a [4], and to optimize H together with a RMS constraint so as to push back the optimal point to the strong DPE region as shown in Fig. 1b. The new objective function becomes

$$J_{\sigma_e^2,RMS} = \sigma_e^2 + \lambda_2[\int |H|^2\, df - p_e], \tag{8}$$

where the first term, σ_e^2, consists of ISI and quantization effects, while the last term is our proposed "RMS control", whose effect is illustrated as green in Fig. 1b. Minimizing $J_{\sigma_e^2,RMS}$, the optimal H becomes

$$H_{\sigma_e^2,RMS}(f) = \frac{C^*(f)S_X(f)}{|C(f)|^2 S_X(f)+\lambda_1 p_c+\lambda_2}. \tag{9}$$

$H_{\sigma_e^2,RMS}$ is still in the form of MMSE for negligible quantization noise ($\lambda_1 = 0$). This form actually gives DPE "RMS awareness" because nonzero λ_2 avoids infinite $H_{\sigma_e^2,RMS}$ when C approaches zero. The second stationary point, i.e, $\partial J_{\sigma_e^2,RMS}/\partial\lambda_2 = 0$ means to solve $\int \left|H_{\sigma_e^2,RMS}(f,\lambda_2)\right|^2 df = p_e$ for λ_2, i.e., filter energy re-normalization, or find λ_2 such that the signal energy from Tx does not exceed the maximum available Tx power, p_e, causing driver nonlinearity. As long as the RMS does not drop too much, the quantization effect does not degrade SNR in the strong DPE region ($\beta > 0.5$) [4], i.e. only an interplay between the ISI control and RMS control is left, shown in Fig. 1b. The quantization noise in $J_{\sigma_e^2,RMS}$ can be discarded ($\lambda_1 = 0$). In this sense, eq. (9) becomes

$$H_{\sigma_e^2,RMS}(f,R_{dB}) = \frac{C^*(f)S_X(f)}{|C(f)|^2 S_X(f)+\lambda_2}, \tag{10}$$

where $R_{dB} = -20\log_{10}\lambda_2$, interpreted as the "depth" measured from the filter top to prevent a near-zero denominator from causing over-enhanced DPE filter magnitudes at high frequencies. The above equation shares the same form as (6) but with different physical meanings. Our derivation and explanation are more self-contained than those in [8].

III. Experimental Results

A four-channel DAC operating at 120 GSample/s and a coherent driver modulator (CDM) were used to generate dual-polarization (DP) 64-QAM modulated signals at 92.31 GBaud and 96 GBaud with a roll-off factor (α) of 0.1 or 0.2 (Fig. 3a). The driver gain was fixed throughout our experiment. The coherent receiver consists of a high-BW ICR and a 160 Gsa/s analog-to-digital converter. DSP was used to recover the signal, including a 35-tap 2×2 complex-valued MIMO and carrier phase recovery. The S21/link response calibration was performed using 4 FIR filters with 255 taps. The measured frequency-domain magnitudes (Fig. 3b) were fed back to the Tx to synthesize DPE filters, $H_{DPE}(f)$, with three different methods. This work studies two cases: back-to-back (B2B), and a link consisting of another six stages of EDFAs and flex wavelength selective switches (WSSs). Fiber is not included in order to eliminate PAPR-induced fiber nonlinearity.

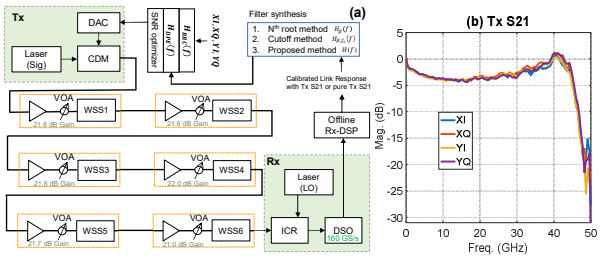

Fig. 3. Experimental setup and the calibrated Tx S21.

In the following, three methods will be compared in Section III.A. Starting off from the B2B, section III.B experimentally demonstrates the RMS restoration of the proposed method. Section III.C examines its sensitivity to parameter R_{dB}. Section III.D re-examines the aboves again in the WSS link (tighter filtering).

A. Different approaches for comparison

In the next few subsections, the proposed method will be compared with the nth root method and the cutoff method using DP-64QAM signals at 92.31GBaud and 96 GBaud. The proposed method always covers the entire signal BW (i.e., ±0.55×B for α = 0.1, ±0.60×B for α = 0.2). For readers' convenience, let us explain the three methods to be compared here.

First, the nth root method employs a DPE filter in the following form:

$$H_\beta(f) = 1/|C(f)|^\beta,\ 0 \le \beta \le 1, \tag{11}$$

where $C(f)$ is the channel response, or experimentally, the DSP-calibrated Tx S21 in frequency domain. As previously discussed, there is no general way to obtain an optimal β, and its optimal values depend on the actual channel response of Tx S21 or WSS link as well as the available RMS of transmitter. An empirical scan in β is therefore required [4].

Second, the cutoff method is defined as the nth root method with the following condition:

$$H_{\beta,f_c}(f) = \begin{cases} H_\beta(f), & \forall |f| \le f_c \\ H_\beta(f_c), & \forall |f| > f_c \end{cases}, \tag{12}$$

where f_c is the one-sided cutoff frequency, beyond which the DPE filter stays the same value as that at f_c. In this paper, f_c is usually taken as 0.48-0.55 for α = 0.1, 0.48-0.60 for α = 0.2, for one-sided DPE. To reduce the RMS due to high -requency enhancement, the above cutoff method was proposed in [4], while other works [5-6, 8] pre-emphasize Tx within signal baudrate only.

To make a fair comparison with the above two methods, we still obtain the nth root of the proposed MMSE filter shape in (10):

$$H(f) = H_{\sigma_e^2,RMS}(f,R_{dB})^\beta,\ 0 \le \beta \le 1. \tag{13}$$

It is expected that the best SNR can be achieved at $\beta = 1$ (full DPE), i.e., equation (13) becomes equation (10).

To avoid over-clipping effect and driver nonlinearity, a digital SNR optimizer is used at TxDSP [4]: the pre-emphasized waveforms, x_t, from the above three methods are multiplied with a digital gain factor, g. The optimal digital

gain is $g_{op,dB} = \max_g \left\{ \langle |x_t|^2 \rangle / \langle \left| \frac{Q(gx_t)}{g} - x_t \right|^2 \rangle \right\} - M_{dB}$, where $Q(\cdot)$ is a 8-bit quantization function with clipping at TxDSP. M_{dB} is a gain margin to avoid driver nonlinearity by sacrificing RMS. M_{dB} is 1dB in this work. This algorithm thus optimizes digital SNR before the DAC for each DPE filter shape, so that the physical driver gain can be set constant.

B. Results for RMS Restoration

Figs. 4 and 5 show the comparison of 92.31G and 96 GBaud DP-64QAM, respectively, between the nth root method with different cutoff frequencies and the proposed method (without cutoff, meaning full bandwidth $\pm(1+\alpha)B/2$). The left and right columns correspond to $\alpha = 0.1$ and $\alpha = 0.2$, respectively.

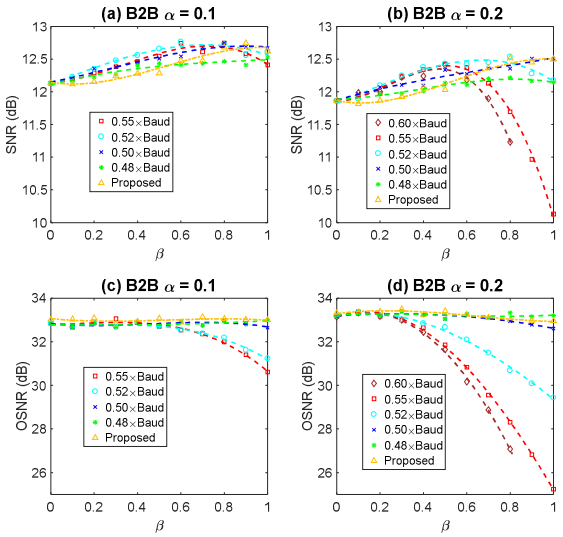

Fig. 4. Comparison between the method "nth root +cutoff" and the proposed method (full-band;0.55×Baud) for pre-emphasizing 92.31 GBaud DP-64QAM in a B2B scenario. The SNRs after Rx DSP for (a) $\alpha = 0.1$ (b) $\alpha = 0.2$, and their availabe OSNRs before Rx DSP for (c) $\alpha = 0.1$ (d) $\alpha = 0.2$.

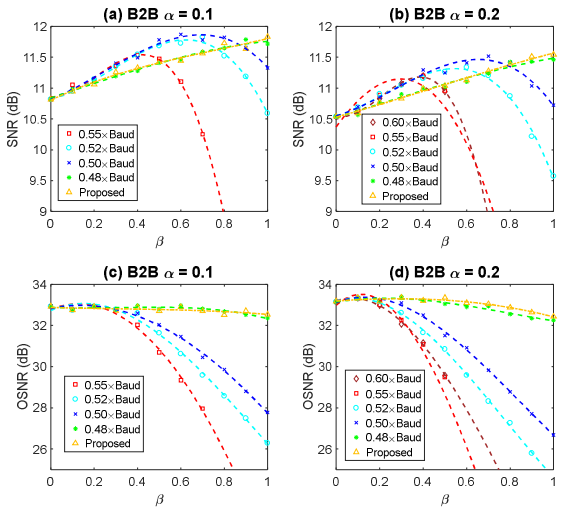

Fig. 5. Comparison between the method "nth root +cutoff" and the proposed method (full-band; 0.60×Baud) for pre-emphasizing 96 GBaud DP-64QAM in a B2B scenario. The SNRs after Rx DSP for (a) $\alpha = 0.1$ (b) $\alpha = 0.2$, and their availabe OSNRs before Rx DSP for (c) $\alpha = 0.1$ (d) $\alpha = 0.2$.

Generally, a smaller α yields better SNR because of less ISI. The optimal β of the full-bandwidth nth root method (red) depends on signal baudrate, α, as well as cutoff frequencies (cyan, blue and green). For 92.31 GBaud, the optimal β's are 0.7 and 0.5 for $\alpha = 0.1$ and $\alpha = 0.2$, respectively, for 96 GBaud, they are 0.4 and 0.3. As discussed in [4], the RMS of the DPE signal decreases more substantially (and thus SNR decreases) when the overall channel, $C(f)$, has a narrower bandwidth.

The RMS reduction of the above three methods can be revealed experimentally by measuring the available OSNR, given a B2B system with fixed parameters, shown in Figs. 4c-d and Figs. 5c-d. The nth root method (red) at full bandwidth causes substantial RMS reduction, and thus OSNR drops significantly in the strong DPE region ($\beta > 0.5$). For example, shown as red in Fig. 5c, the available OSNR of 96 GBaud 64 QAM ($\alpha = 0.1$) drops from 33 dB to 25 dB for B2B, which justifies that the RMS control is indispensable in our proposal.

In order to push back the optimal point to the strong DPE region, the recently proposed cutoff method helps reducing RMS loss [4]. The best cutoff frequencies, f_c, are 0.50×B for 92.31 GBaud shown as blue in Figs. 4a-b and 0.48×B for 96 GBaud shown as green in Figs. 5a-b, all at $\beta = 1$. Higher signaling rates require a smaller cutoff ratio (0.48 compared to 0.50) since more pre-emphasis on high frequency components is required to combat ISI, resulting in a larger PAPR that shrinks the RMS. However, generally, the cutoff method contains two parameters for optimization. For example, other than $\beta = 1$, another optimal f_c for 92.31 GBaud ($\alpha = 0.1$) is 0.52×B at $\beta = 0.7$, shown as cyan in Fig. 4a. Thus, either partial or full DPE can achieve optimal SNR using this method.

To further achieve a full DPE, i.e., $\beta = 1$, our proposal, presented as dashed orange, increases SNR as β gets larger, and attains the best SNR at $\beta = 1$ without suffering from substantial RMS loss. Note that our proposed method is a full-signal-BW DPE, without any frequency cutoff. Shown as orange in Figs. 4 and 5, both cutoff method and the proposed method have a similar performance at $\beta = 1$, and the best achievable SNRs are 0.3-0.4dB better than the nth root method (red).

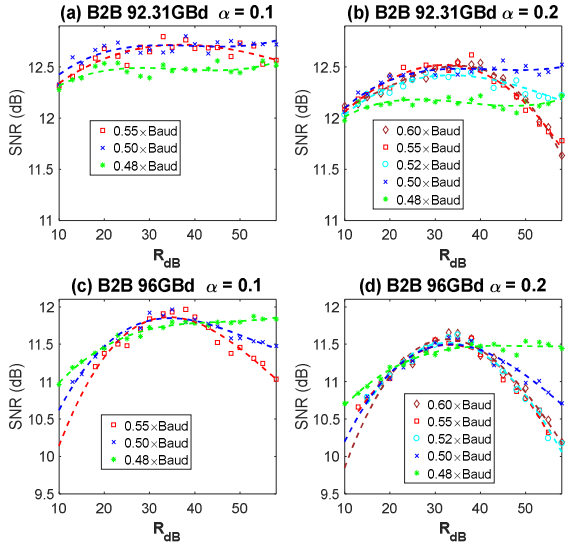

Fig. 6. Sensitivity to parameter R_{dB} of the proposed method with different cutoff frequencies. (a) $\alpha = 0.1$ (b) $\alpha = 0.2$ for 92.31 GBaud (c) $\alpha = 0.1$ (d) $\alpha = 0.2$ for 96 Gbaud.

C. *Insensitivity to parameter R_{dB}*

In the previous section, R_{dB} was chosen to be 30dB for SNR maximization at $\beta = 1$. For productization, the optimal R_{dB} will be pre-calculated given a factory-calibrated Tx S21. This section examines if the proposed method is sensitive to R_{dB} since S21 may vary due to aging or power reboot. Additionally, in order to investigate if the cutoff method may lessen or worsen the sensitivity to R_{dB}, a cutoff method is added on top of the proposed method, $H_{\sigma_e^2,RMS}(f, R_{dB})$, in (10):

$$H(f) = \begin{cases} H_{\sigma_e^2,RMS}(f, R_{dB}), \forall |f| \le f_c, \\ H_{\sigma_e^2,RMS}(f_c, R_{dB}), \forall |f| > f_c \end{cases}. \quad (14)$$

The parameter sensitivity is presented as SNR versus R_{dB} in Fig. 6a-b for 92.31 GBaud and in Fig. 6c-d for 96 GBaud. The proposed method without cutoff is shown as red ($f_c = 0.55 \times$ B) for $\alpha = 0.1$ and as brown ($f_c = 0.60 \times$ B) for $\alpha = 0.2$. Generally, 92.31 GBaud suffers less from the tight filtering of S21, and its SNR changes more gently over R_{dB} than 96 GBaud. Similarly, at the same baudrate, a smaller α, or smaller signal bandwidth, is less sensitive to R_{dB}. The proposed method equipped with the cutoff method, say, $f_c = 0.48 \times$ B, shown as green, may help lessen the sensitivity to R_{dB}, but the SNR also decreases due to more ISI.

For both baud rates, R_{dB} can be taken between 30 and 35 dB without too much SNR variation. This eases our filter design in a sense that, given a calibrated Tx s21, only a single, insensitive parameter is required to provide a robust DPE compared to other schemes [4-7] requiring a parameter scan in (β, f_c). Another question is, should we choose 30dB or 35dB? In the presence of WSS filtering with only DPE for Tx S21, the power loss due to WSS suppression causes substantial amount of SNR degradation. For R_{dB}= 35 dB, high frequency signal components are more enhanced, resulting in a larger decrease in the overall signal RMS (power). The WSS filtering suppresses signal edges which contain relatively more power. Thus, R_{dB} should be smaller to reduce RMS loss, since the available signal power could be higher after passing through the WSSs, which will be experimentally verified in the next subsection.

D. *WSS filtering*

The proposed method was examined with a link with six 100GHz wide WSSs: Here only one-sided DPE in frequency domain and one-sided calibration of the overall link response were considered to emulate the practical scenario of low DSP complexity. Since WSS priors may not be available in a link (in case that optical feedback is absent), the scenario of purely pre-emphasizing Tx s21 was also investigated for comparison here. Fig. 7a and Fig. 7b are the DPE performances for pre-emphasizing the entire link and pre-emphasizing only Tx S21, respectively, given the overall link response, shown in Fig. 8b, characterized using 4 real FIR filters with 255 taps, as previously discussed at the beginning of Section III. There was an overall offset of 1GHz measured from the optical spectrum of the link, which, however, was not revealed from the one-sided calibration and one-sided DPE. The sensitivity analysis of the DPE for the entire link and for only the Tx are shown as blue and red, respectively, in Fig. 8.

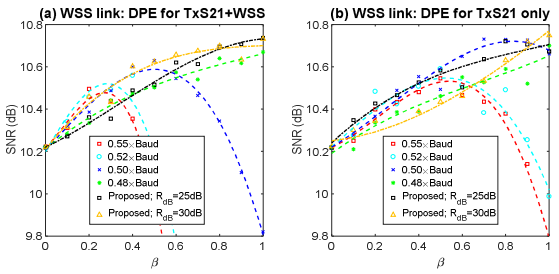

Fig. 7. Comparison between the method "nth root + cutoff" and the proposed method (full-band; 0.55×Baud) for pre-emphasizing 92.31 GBaud DP-64QAM only using the responses of (a) the Tx S21 and six WSSs (b) only the Tx S21.

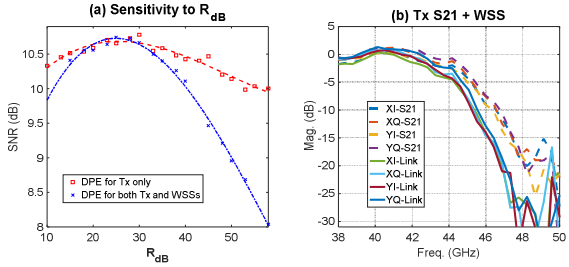

Fig. 8. (a) The proposed method's sensitivity to R_{dB}. (b) Pure Tx S21, and the entire link response (Tx S21 and WSSs).

In both scenarios, compared to a B2B in Fig. 6, the optimal R_{dB} reduces from around 30 dB (Fig. 6) to around 25 dB (Fig. 8a). Compared to B2B, WSS filtering narrows the bandwidth of the channel $C(f)$, leading to a smaller R_{dB} (or a larger λ_2), such that the RMS control receives more "weight" in (8). The best SNR values of both cases are similar, while the advantage of pre-emphasizing only Tx s21 is that the sensitivity to R_{dB} can be reduced, shown as red in Fig. 8a. One could pick either 25 or 30 dB without much SNR variation, in this example. The proposed method, shown as orange and black in Figs. 7a and 7b, always achieves the best SNR for full DPE (β= 1), such that ISI can be minimized before the Rx DSP.

Comparing the best SNRs from both scenarios, pre-emphasizing the entire link may not enhance too much the performance for two reasons. First, WSSs result in tighter filtering, and thus the DPE will suffer more from RMS loss. Second, an accurate extraction of link response (with sufficient resolution) is required, plus the low-complexity DSP only allows one-sided DPE (symmetric) for optical filtering with WSS offsets (asymmetric spectrum).

IV. Conclusion

In this work, we design a DPE filter based on ISI, RMS and ENoB, which are optimized together with a RMS constraint so as to push back the optimal point to the strong pre-emphasis region.

The nth root method causes substantial RMS loss and thus partial DPE is necessary. Together with a cutoff method, RMS can be restored but the optimal point may require two-dimensional parameter search, depending on the channel response. The proposed method provides a mathematical interpretation to shape the high-frequency content of the pre-emphasized signal, i.e., the proposed DPE covers the entire signal bandwidth (no cutoff is required). Experiments show that the proposed method achieves the best SNR for full DPE (β = 1), such that the ISI can be minimized before Rx DSP. Moreover, the proposed method is not sensitive to the single parameter, R_{dB}. Hence, the optimal R_{dB} can be pre-calculated

given a factory-calibrated Tx S21 for productization, and will not change much the performance due to aging or power reboot.

Finally, pre-emphasizing the entire link may not offer a much better performance than pure for Tx S21 for two reasons. First, WSSs result in tighter filtering and thus the DPE will suffer more from RMS loss. This also makes the proposed method more sensitive to parameter R_{dB}. Second, an accurate extraction of link responses (with sufficient resolution) is required, plus the low-complexity DSP only allows one-sided DPE (symmetric) for optical filtering with WSS offsets (asymmetric spectrum).

Other than ISI and RMS, more constraints can be used for optimization. This, however, affects the robustness of the design since more effort is required for parameter search, and the design becomes more sensitive to more parameters.

REFERENCES

[1] D. Rafique, et al., "Digital preemphasis in optical communication systems: On the DAC requirements for terabit transmission applications," IEEE J. Lightwave Technol., vol. 32, no. 19, pp. 3247-3256 (2014).

[2] Z. Zhou et al., "Impact of Analog and Digital Pre-Emphasis on the Signal-to-Noise Ratio of Bandwidth-Limited Optical Transceivers, " IEEE Photonics Journal, vol. 12, no. 2, pp. 1-12 (2020).

[3] Y. Zhao et al., "A Novel Analytical Model of the Benefit of Partial Digital Pre-Emphasis in Coherent Optical Transponders," ECOC (2020).

[4] W. C. Ng et al., "Low-Complexity RMS-enhanced Digital Pre-emphasis under Limited Transmitter Power and ENoB", Proc. OFC, W2A.27 (2023).

[5] S. T. Le and J. Cho, "OSNR-Aware Digital Pre-Emphasis for High Baudrate Coherent Optical Transmissions," Proc. OFC, M3H.4 (2022).

[6] Y. Mori, H. Hasegawa, and K. Sato, "Joint pre-, inline-, and post-compensation of spectrum narrowing caused by traversing multiple optical nodes," in Proc. Eur. Conf. Opt. Commun., Paper P1.SC3.45 (2017).

[7] Z. Qiang and Y. Hong, "PAPR Constrained Digital Pre-emphasis for Short-reach Coherent Systems with Transmitter Bandwidth Limitation," Proc. ACP (2022).

[8] A. Napoli et al., "Digital Compensation of Bandwidth Limitations for High-Speed DACs and ADCs," J. Lightwave Technol. 34(13), 3053–3064 (2016).

[9] J. Pan and S. Tibuleac, "Real-time ROADM filtering penalty characterization and generalized precompensation for flexible grid networks," IEEE Photon. J. 9, 7202210 (2017).